Detection of Histone Modifications at Specific Gene Loci in Single Cells in Histological Sections

Delphine Gomez; Laura L Shankman; Anh T Nguyen; Gary K Owens.

Supplementary Figures 1-13

Supplementary Table 1

Supplementary Figure 1: Compatibility between PLA and chromatin structure.

a

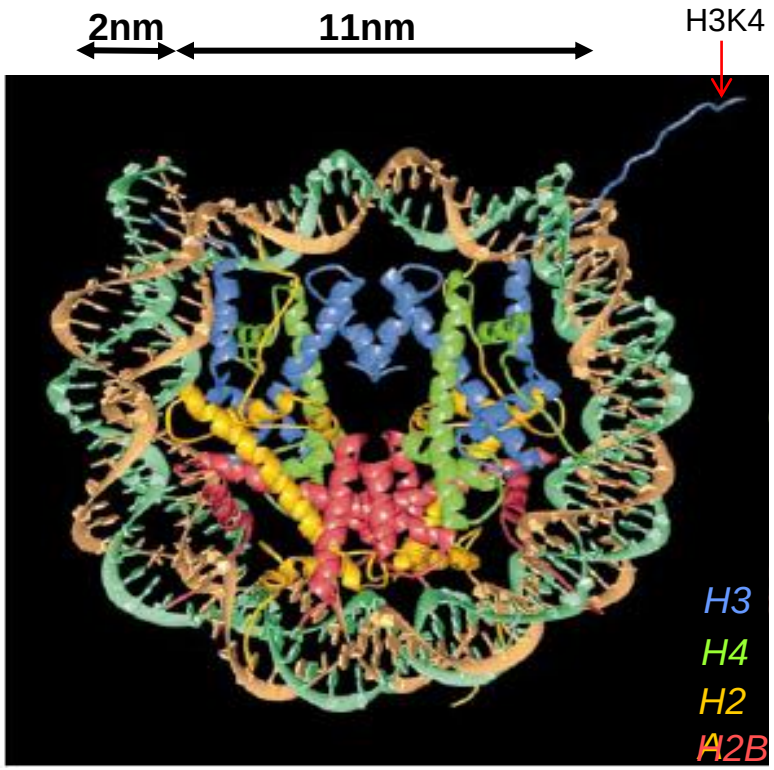

Estimated distance between two biotinylated ATPs within the DNA strand ~2 nm

b

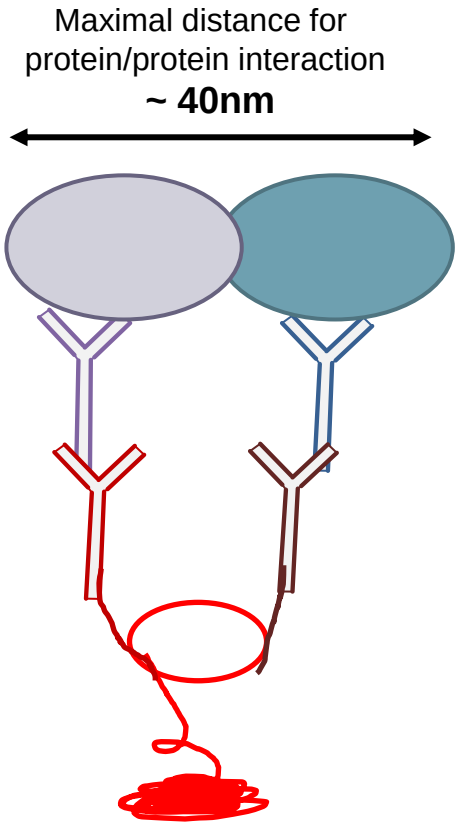

(**a**) Reprinted partially from Luger *et al. Nature* 1997 389:251-260 (reproduced with permission: 3020231289008). The diameter of the nucleosome and the DNA double strand helix is approximatly 11 nm and 2 nm, respectively. The distance between two biotinylated ATPs within the DNA strand is estimated to be 2 nm. (**b**) Together, these estimates establish the feasibility of PLA for the detection of H3K4dime on the *MYH11* promoter based on the maximal distance of 40 nm between two entities that can be detected by PLA.

Supplementary Figure 2: Pepsin treatment does not affect H3K4dime staining in tissue sections.

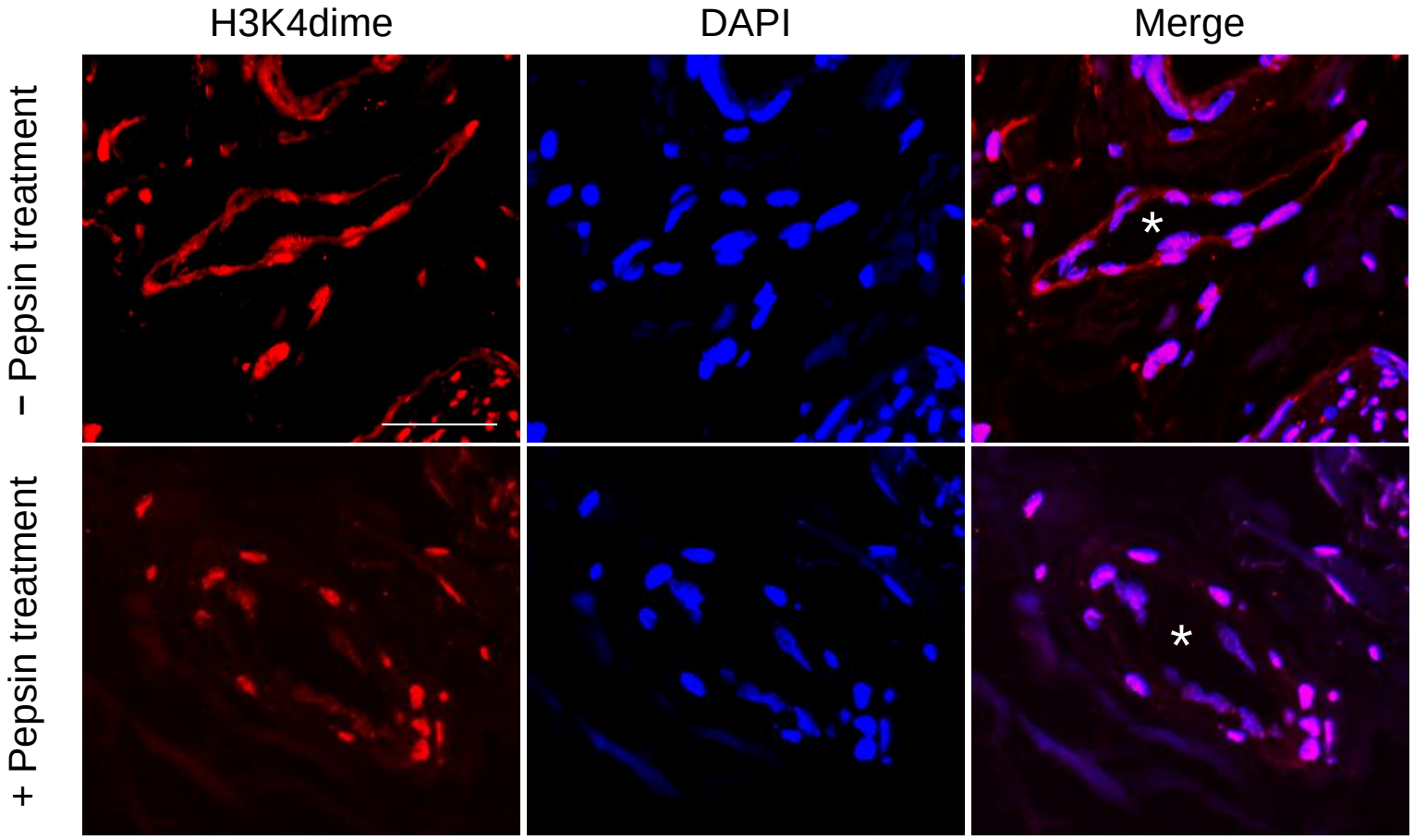

Immunostaining of H3K4dime (red) in the adventitia of formalin-fixed paraffin-embedded (FFPE) human coronary arteries with and without pepsin treatment. The adventitial layer consists of fibroblasts and small vessels containing SMCs and ECs. These vessels were identified with a star corresponding with the lumen of the vessel (*). Nuclear H3K4dime staining is similar in all cell types within the adventitia and remains unchanged after pepsin treatment and ISH procedure. Scale Bar = 50 µm.

Supplementary Figure 3: Mapping of H3K4dime enrichment on the MYH11 promoter.

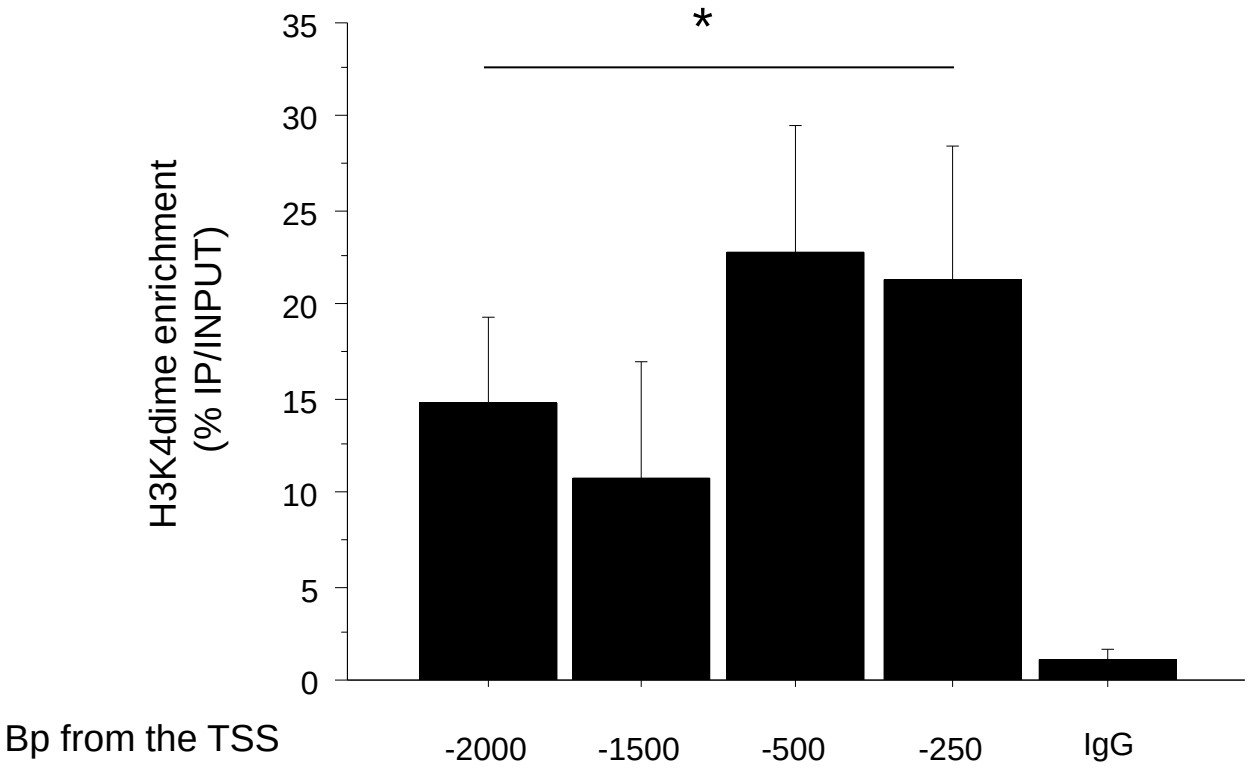

Conventional ChIP assay of H3K4dime on the *MYH11* promoter in cultured SMCs. H3K4dime enrichment was assessed along the *MYH11* promoter between the transcription start site (TSS) and –2000 base pairs. A significant enrichment of H3K4dime is quantified on the *MYH11* promoter region chosen for *MYH11* probe design compared with control IgG. Error bars = s.d.; n = 3 independent experiments; * $P < 0.005$.

Supplementary Figure 4: Y chromosome FISH in male patient tissue sections.

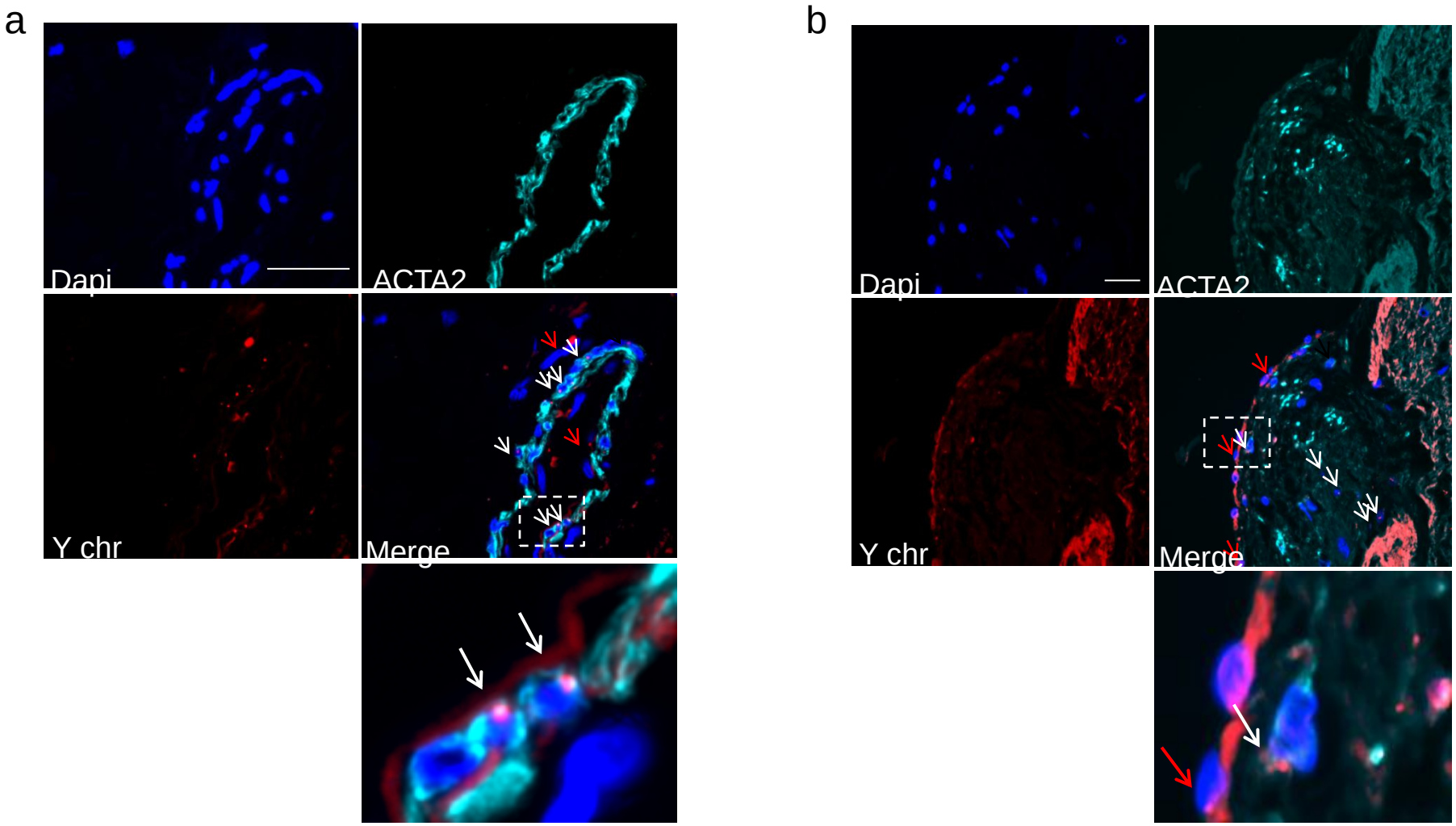

Fluorescent *In Situ* Hybridization (FISH) in FFPE carotid samples from male patients using a Red-dUTP labeled probe designed for hybridization with human Y chromosome (clone RP11-88F4). Y chromosome probe hybridization was analyzed in small vessels within the adventitia (**a**) and in large carotid arteries (**b**). Red spots corresponding with Y chromosome probe hybridization is visualized in small and large vessels with similar hybridization efficiencies within SMCs (white arrows) and ECs (red arrows) providing validation of the ISH protocol. The efficiency of detection or the Y-chromosome was estimated to be 64%, which is similar to the overall efficiency of our ISH-PLA assays. Scale bar = 50 µm.

Supplementary Figure 5: Assessment of H3K4dime enrichment at *MYH11* promoter in various cultured cell lines.

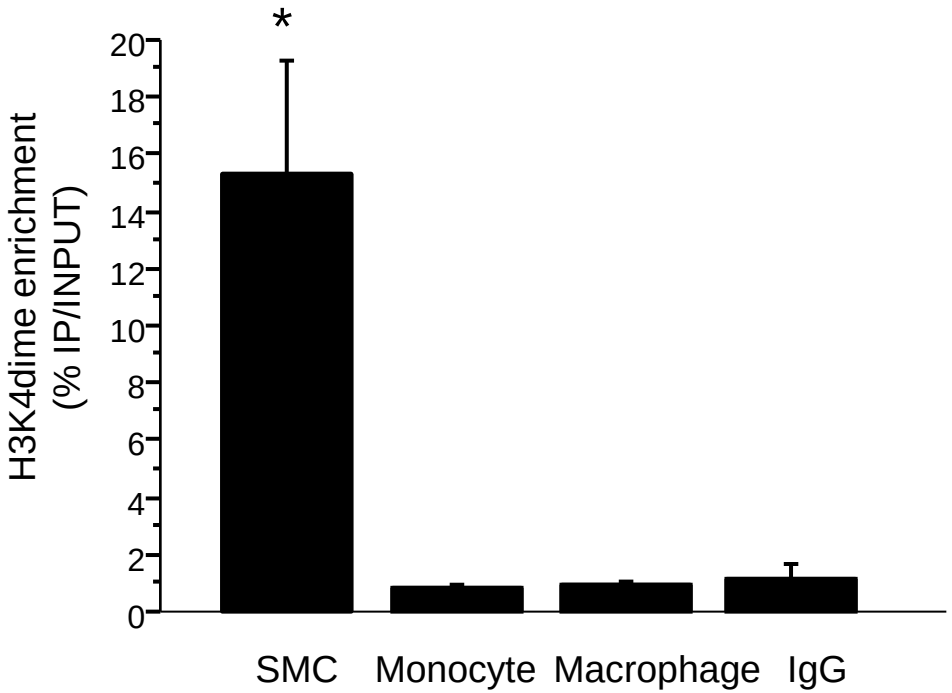

Conventional ChIP assays were performed in SMC, macrophage and monocyte cell lines. The absence of H3K4dime on *MYH11* in monocyte and macrophage cell lines further extends results showing that *MYH11* H3K4dime is a specific mark of SMC lineage. Data represent means ± s.d.; *n* = 3 independent experiments; * *P* < 0.001 *vs* IgG control.

Supplementary Figure 6: Assessment of eYFP expression in *Myh11 Cre*ER^{T2} ROSA26 STOP flox eYFP$^{+/+}$ and eYFP$^{-/-}$ mice.

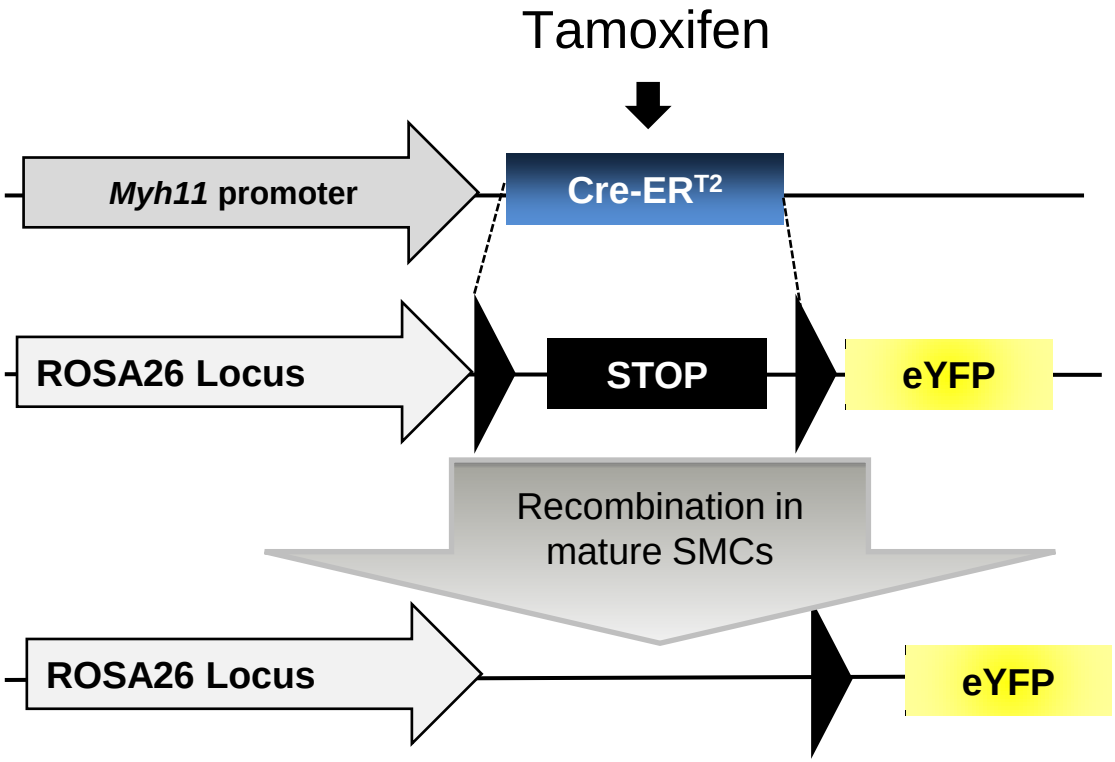

(**a**) SMC lineage tracing was done by crossing *Myh11*-CreER^{T2} transgenic mice with ROSA26 STOP flox eYFP$^{+/+}$ mice and treating mice with tamoxifen between six and eight weeks of age thereby providing SMC-specific and permanent lineage tagging of SMCs with eYFP.

Supplementary Figure 6: Assessment of eYFP expression in *Myh11 Cre*ER^{T2} ROSA26 STOP flox eYFP$^{+/+}$ and eYFP$^{-/-}$ mice.

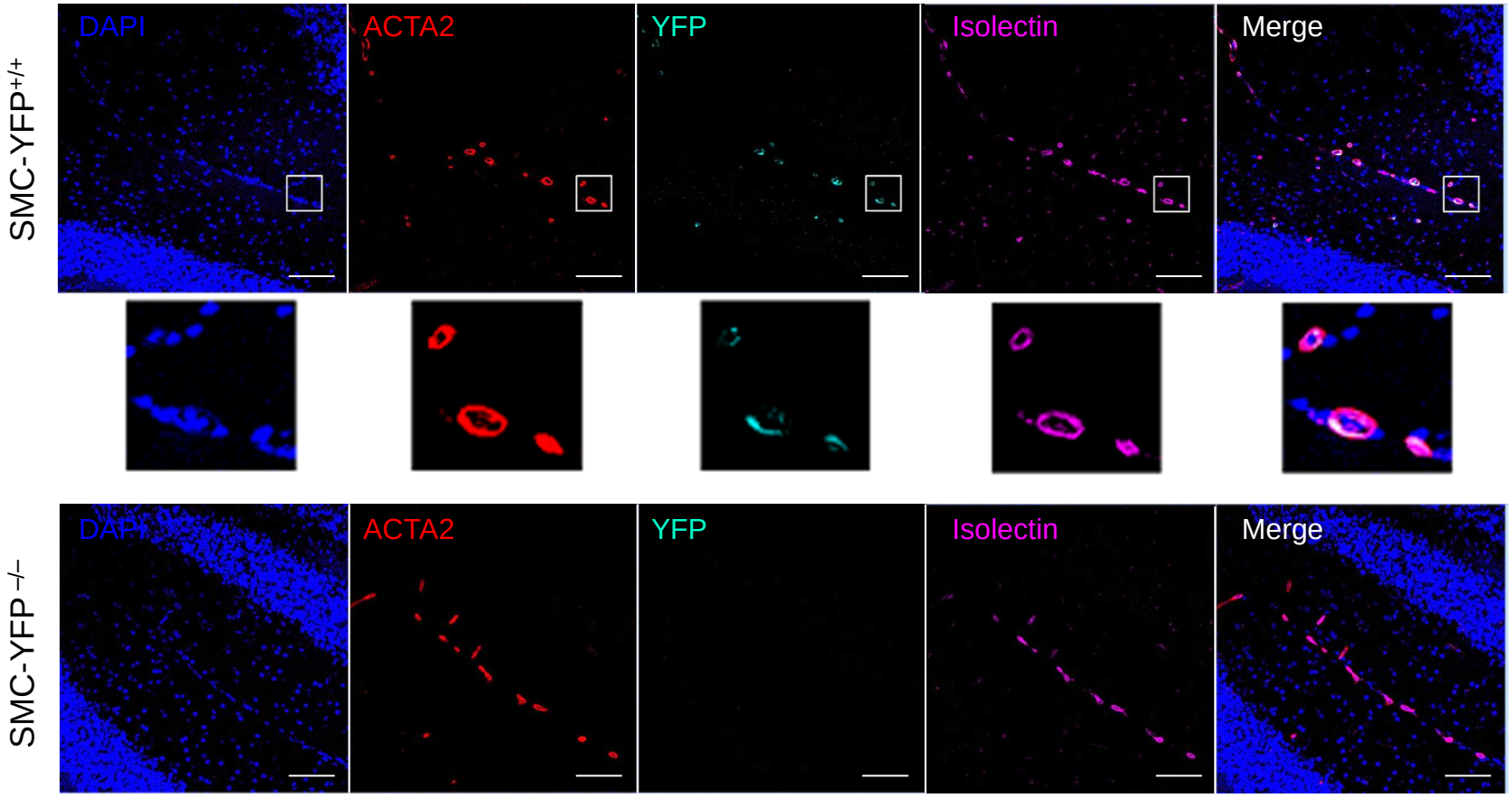

(**b**) Assessment of eYFP expression in cerebellum tissue sections of *Myh11 Cre*ER^{T2} ROSA26 STOP flox eYFP$^{+/+}$ and eYFP$^{-/-}$ mice by immunostaining for eYFP (cyan), ACTA2 (red), isolectin (purple) and Dapi (blue). eYFP staining was observed in eYFP$^{+/+}$ mice whereas no eYFP staining was detected in eYFP$^{-/-}$ mice. Scale bar = 100 µm.

Supplementary Figure 6: Assessment of eYFP expression in *Myh11 Cre*ER^{T2} ROSA26 STOP flox eYFP$^{+/+}$ and eYFP$^{-/-}$ mice.

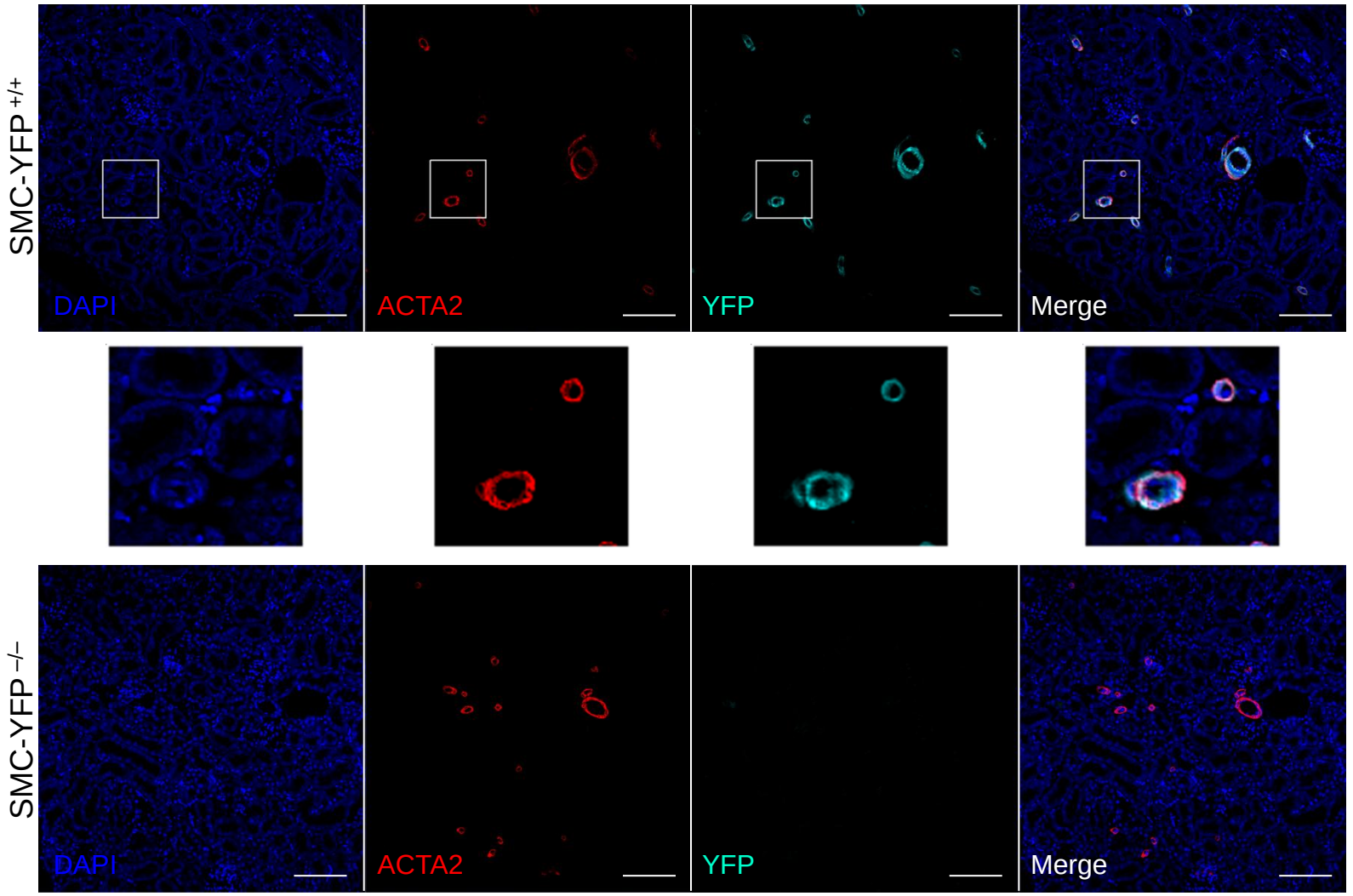

(**c**) Assessment of eYFP expression in kidney tissue sections of *Myh11 Cre*ER^{T2} ROSA26 STOP flox eYFP$^{+/+}$ and eYFP$^{-/-}$ mice by immunostaining for eYFP (cyan), ACTA2 (red), isolectin (purple) and Dapi (blue). eYFP staining was observed in eYFP$^{+/+}$ mice whereas no eYFP staining was detected in eYFP$^{-/-}$ mice. Scale bar = 100 µm.

Supplementary Figure 6: Assessment of eYFP expression in *Myh11 Cre*ER^{T2} ROSA26 STOP flox eYFP$^{+/+}$ and eYFP$^{-/-}$ mice.

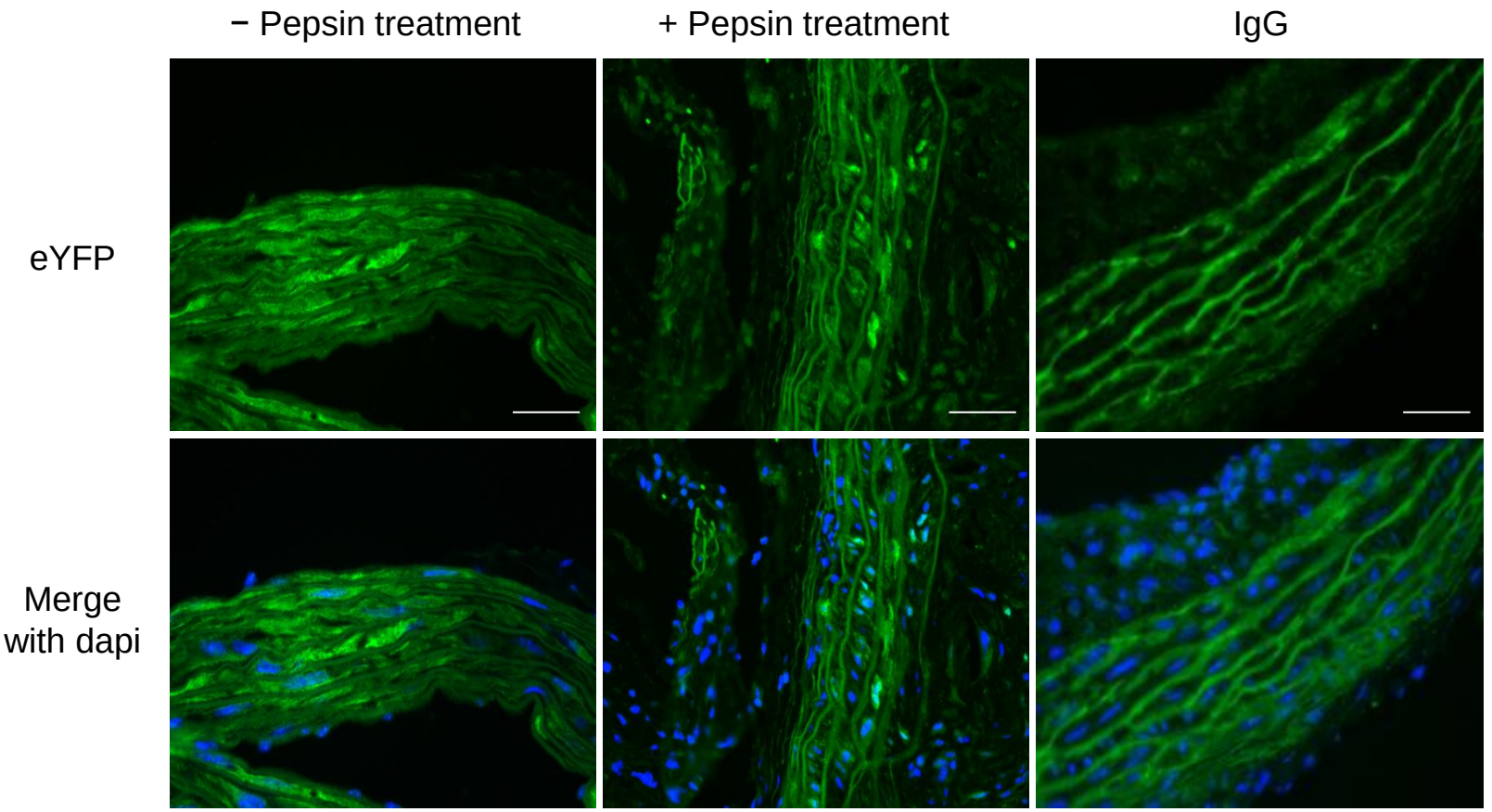

(**d**) The reliability of the eYFP staining (green) with and without pepsin treatment was assessed in aorta tissue sections. eYFP detection was preserved after pepsin treatment. Scale bar = 10 µm.

Supplementary Figure 7: Quantification of ISH-PLA efficiency.

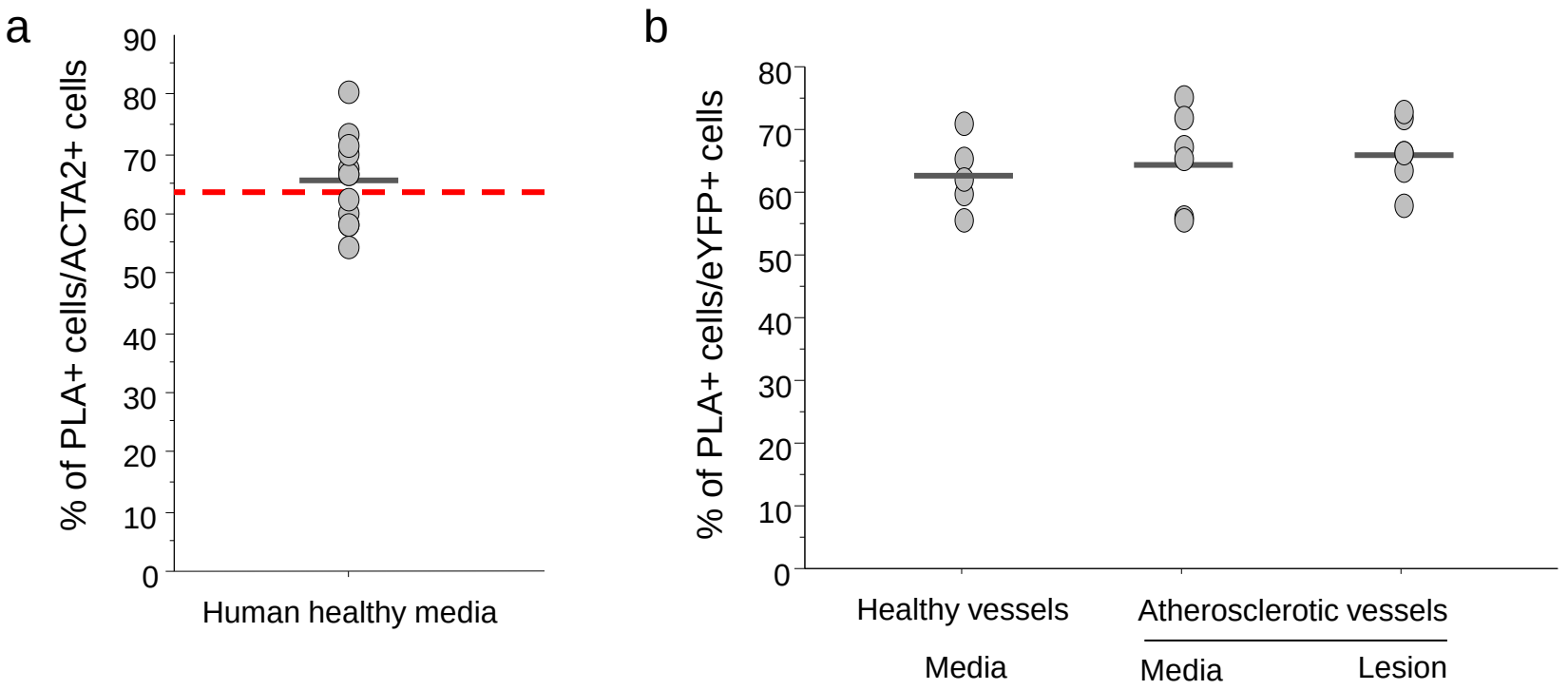

(**a**) Percentage of *MYH11* H3K4dime PLA+ cells/ACTA2+ medial cells detected by ISH-PLA in healthy human vessels. Results indicate that approximately 66% (grey line) of ACTA2+ medial cells are detected (PLA+) by ISH-PLA. The efficiency of ISH-PLA is compared with the estimated efficiency of the FISH procedure (64%, red line) based on our Y-chromosome FISH analyses on parallel histological sections (data presented in **Supplementary Fig. 4**). (**b**) Percentage of Myh11 H3K4dime PLA+ cell/eYFP+ cells detected by ISH-PLA in brachiocephalic arteries of SMC-eYFP$^{+/+}$ mice. The ISH-PLA efficiency was 63% in healthy BCA of SMC-eYFP$^{+/+}$ mice, 65% in the media of atherosclerotic BCA, and 67% in the lesion of atherosclerotic BCA of SMC-eYFP$^{+/+}$-ApoE$^{-/-}$ mice. Mean, s.d and *n* for these quantifications are indicated in **Supplementary Fig. 4c**).

Supplementary Figure 7: Quantification of ISH-PLA efficiency.

c

Species	Samples	Method	Target gene	Nb of sections	Mean (%)	St Dev
Human	Healthy vessels	ISH/PLA	*MYH11* (H3K4dime)	15	66	0.7
Human	Healthy vessels	FISH	Y chromosome	5	64	0.8
Mouse	Healthy vessels	ISH/PLA	*Myh11* (H3K4dime)	7	63	0.6
Mouse	Atherosclerotic vessel: media	ISH/PLA	*Myh11* (H3K4dime)	6	65	0.8
Mouse	Atherosclerotic vessel: lesion	ISH/PLA	*Myh11* (H3K4dime)	6	67	0.6

(**c**) Table summarizing quantitative analyses including the number of sections, the means of the percentage of PLA+ cells/ACTA2+ cells for human specimens, or the percentage of PLA+ cells/eYFP+ cells for SMC-eYFP$^{+/+}$ mouse specimens.

Supplementary Figure 8: *CDH5* H3K4dime PLA in human and mouse tissue sections.

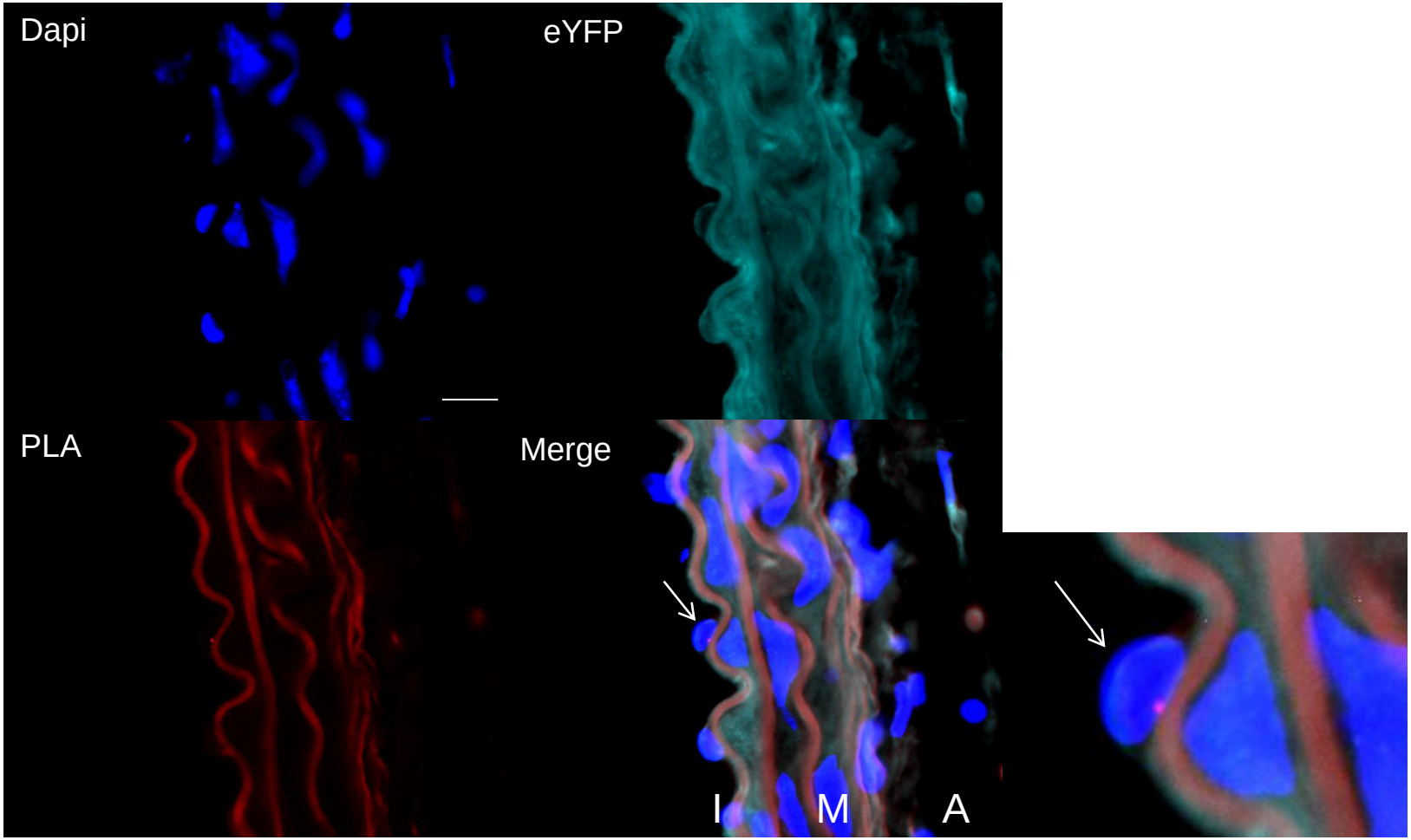

(**a**) Results of *Cdh5* H3H4dime ISH-PLA assays in paraformaldehyde-fixed paraffin embedded histological sections of the brachiocephalic arteries (BCA) from SMC-eYFP$^{+/+}$ mice. PLA+ signals (red dots) were exclusively observed in Endothelial Cells (ECs) lining the lumen of the blood vessel intima (I) (arrow). In contrast, no PLA signal was detected in eYFP+ SMCs in the media (M) or in fibroblasts of the adventitia (A). Scale bar = 10 µm.

Supplementary Figure 8: *CDH5* H3K4dime PLA in human and mouse tissue sections.

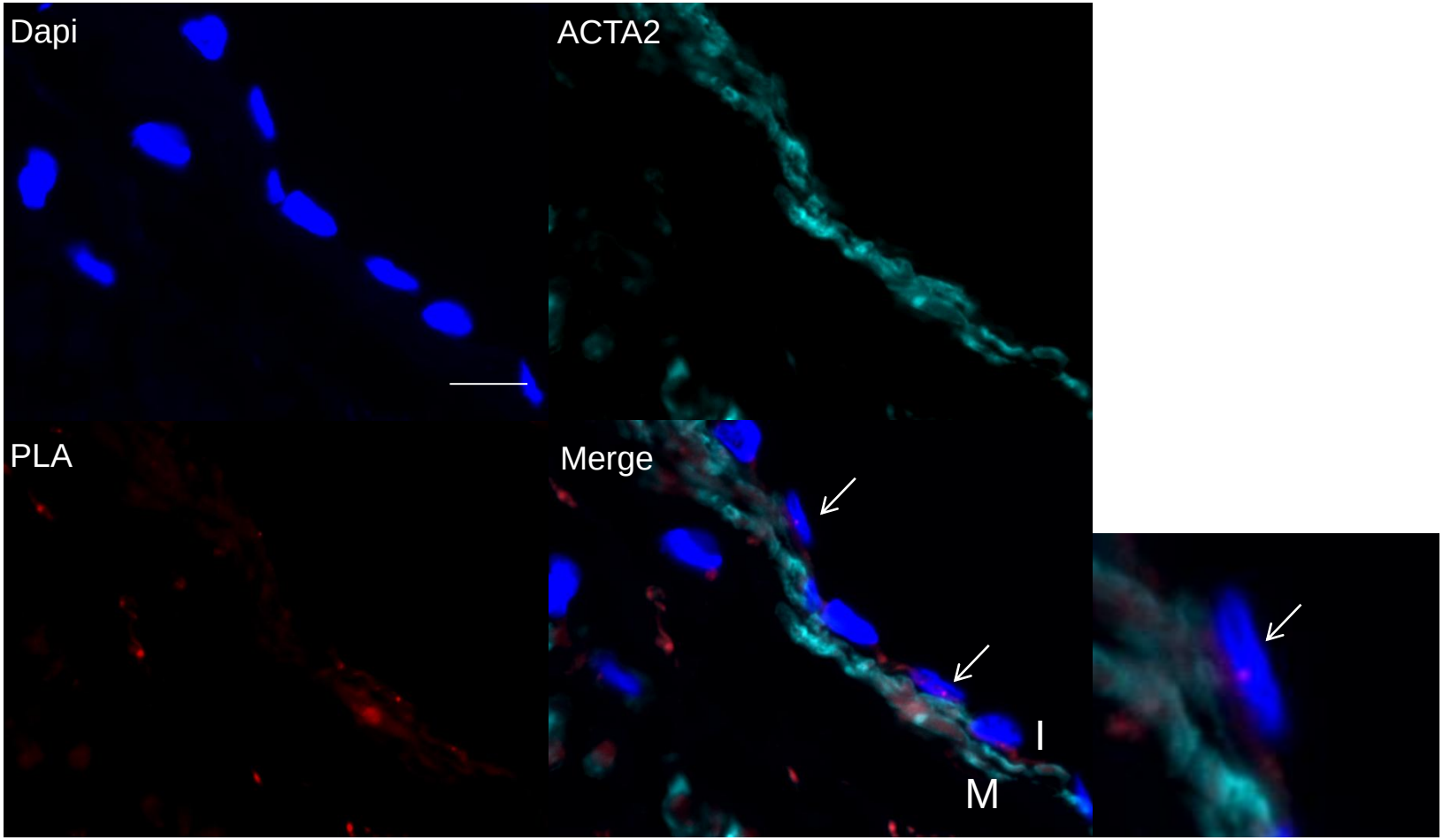

(**b**) Similar *CDH5* H3K4dime PLA assays were performed in FFPE human carotid arteries. *CDH5* H3K4dime PLA+ cells were strictly found within the intimal layer (I) and correspond to ECs (arrows). No medial SMCs (M) were PLA+. Scale bar = 10 µm.

Supplementary Figure 9: *Tagln* H4ac PLA in mouse tissue sections.

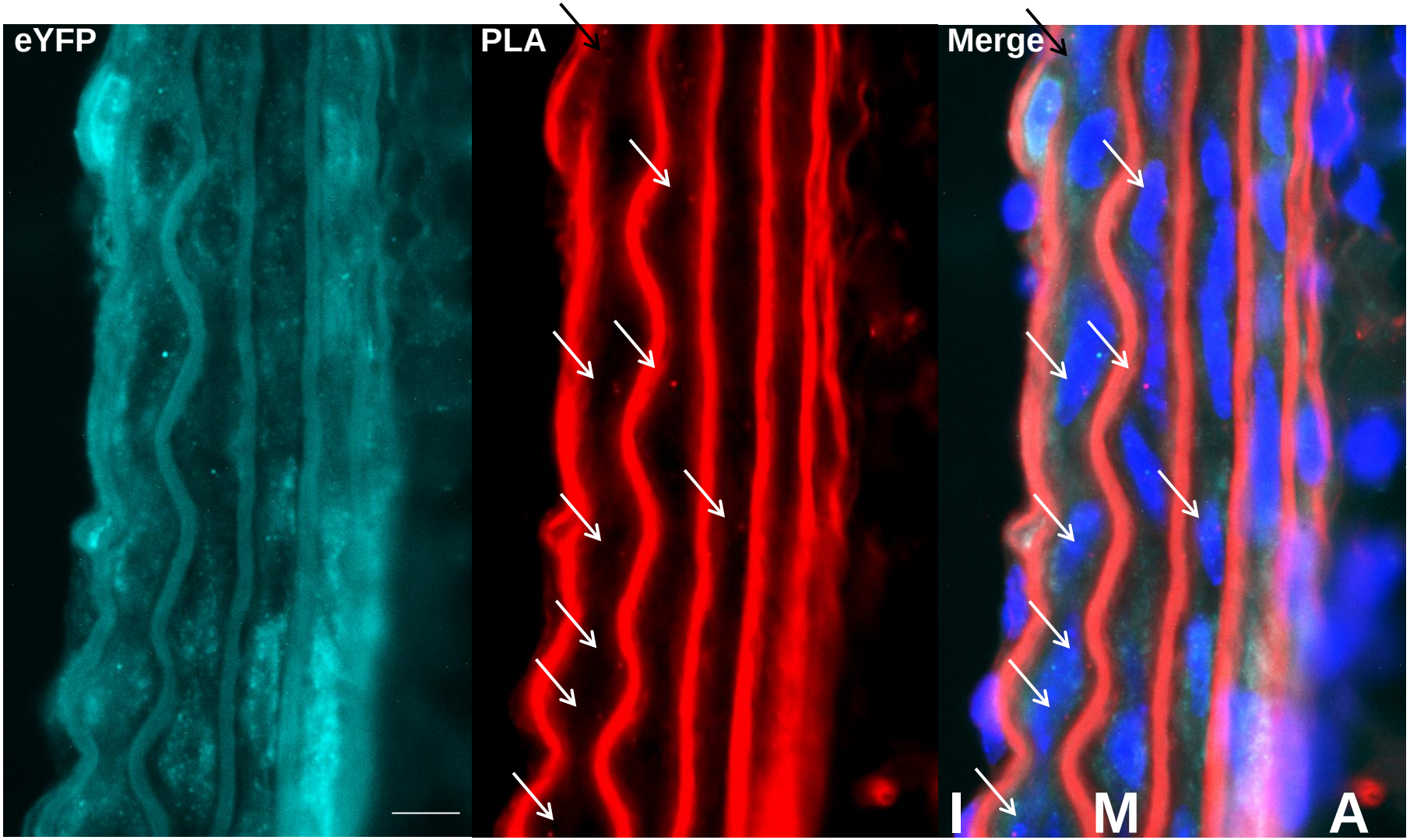

(**a**) Results of *Tagln* H4ac ISH-PLA assays in BCA sections from SMC-eYFP$^{+/+}$ mice. Results showed that a large fraction of eYFP+ medial SMC were *Tagln* H4ac PLA+ (media, M) whereas ECs (intima, I) and advential cells (Adventitia, A) were negative. Scale bar = 10 µm.

Supplementary Figure 9: *Tagln* H4ac PLA in mouse tissue sections.

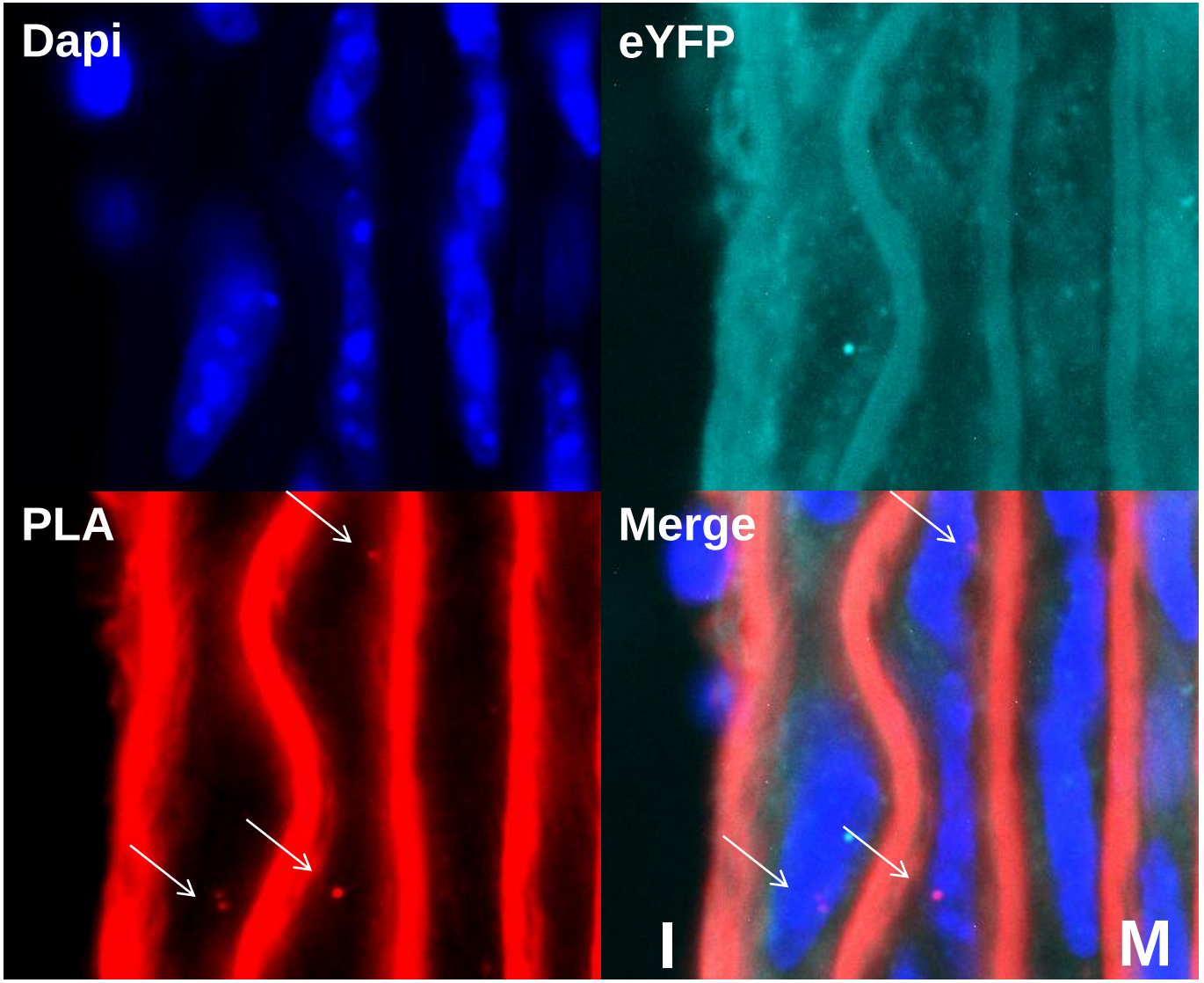

(**b**) Zoom in corresponding to the previous images (**Supplementary Fig. 9a**) focused on *Tagln* H4ac PLA+/eYFP+ SMCs (Arrows).

Supplementary Figure 10: *MYH11* H3K4dime ISH-PLA assay in FFPE human carotid arteries.

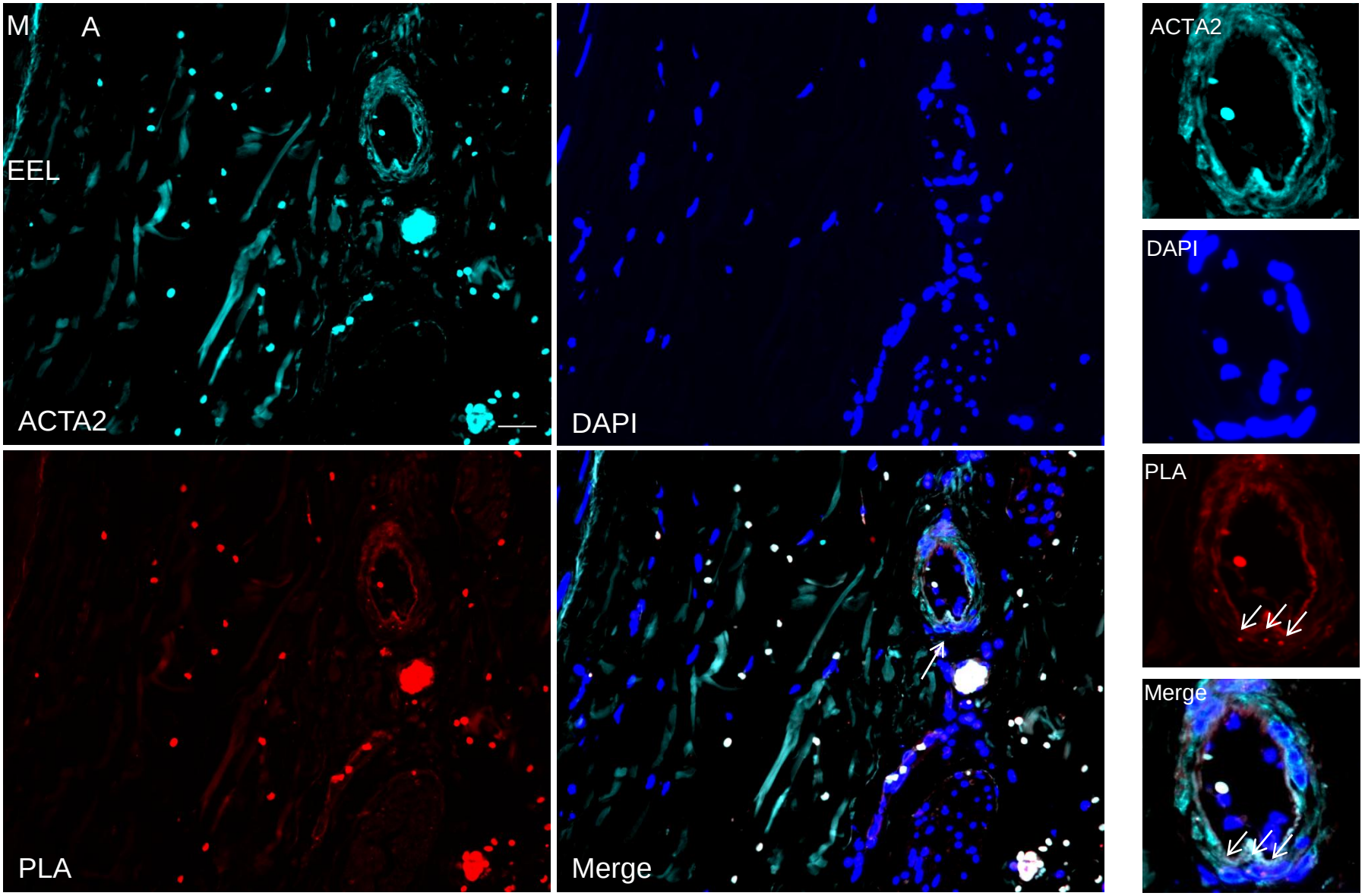

General view of the adventitia showing PLA+ signal only in SMCs associated with small vessels (arrows). Staining for ACTA2 (cyan), PLA (red), Dapi (blue) and merge of images. Scale bar = 50 µm. Higher magnification of the main image is shown in the right panels centered on an adventitial vessel.

Supplementary Figure 11: *MYH11* H3K4dime ISH-PLA assay in FFPE human brain sections.

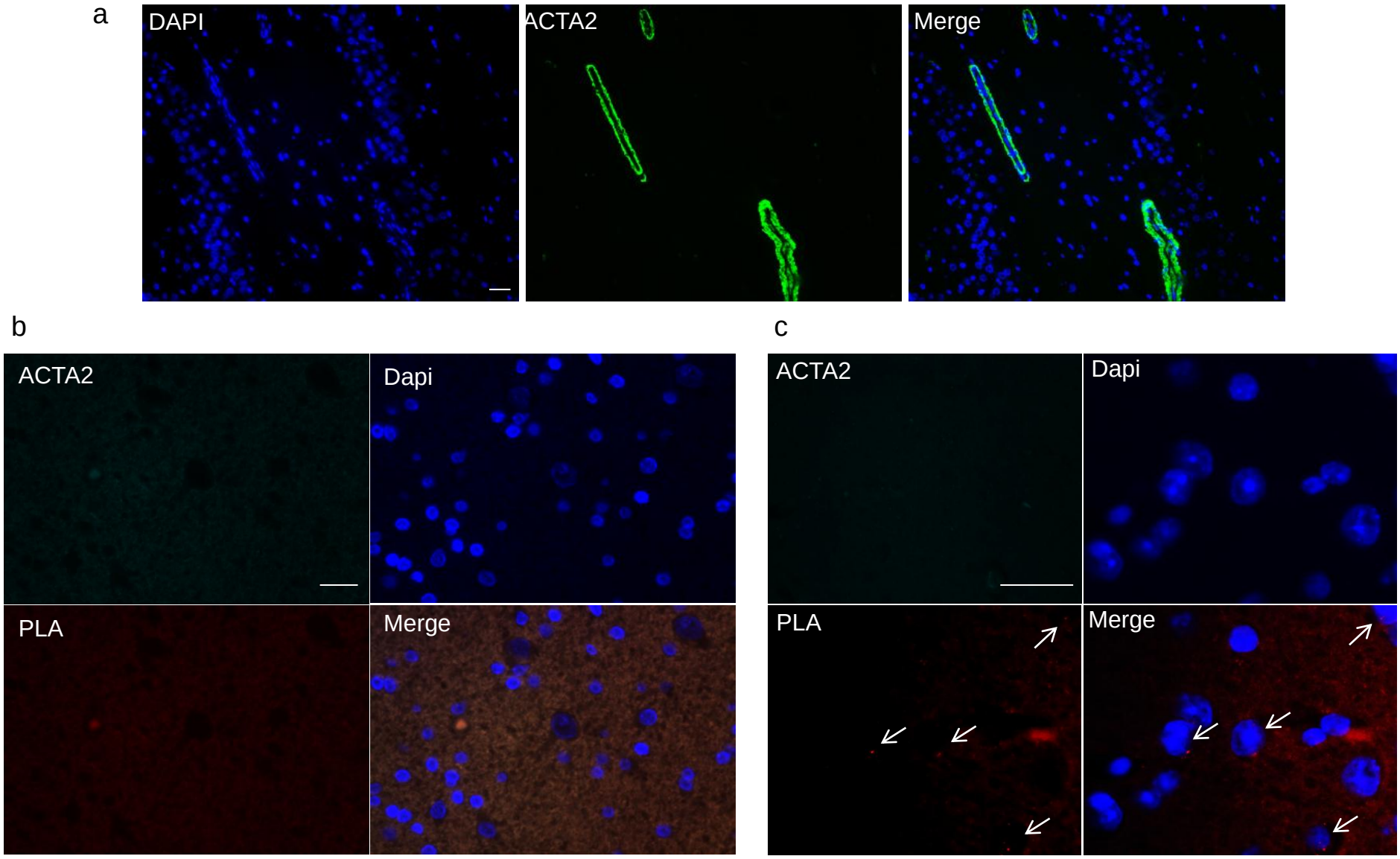

(**a**) A general view of brain sections showing the presence of vessels including ACTA2+ SMCs. Scale bar = 100 µm. (**b**) Non-SMC cells within the brain (ACTA2-) are strictly *MYH11* H3K4dime PLA–. (**c**) In contrast, non-SMCs within the brain are *MYH11* H3K27trime PLA+ (arrows), similar to observations in ECs (**Fig. 3d**). Scale bars for (**b**) and (**c**) = 10 µm.

Supplementary Figure 12: Immunofluorescent staining of SMC marker proteins in healthy and atherosclerotic human carotids.

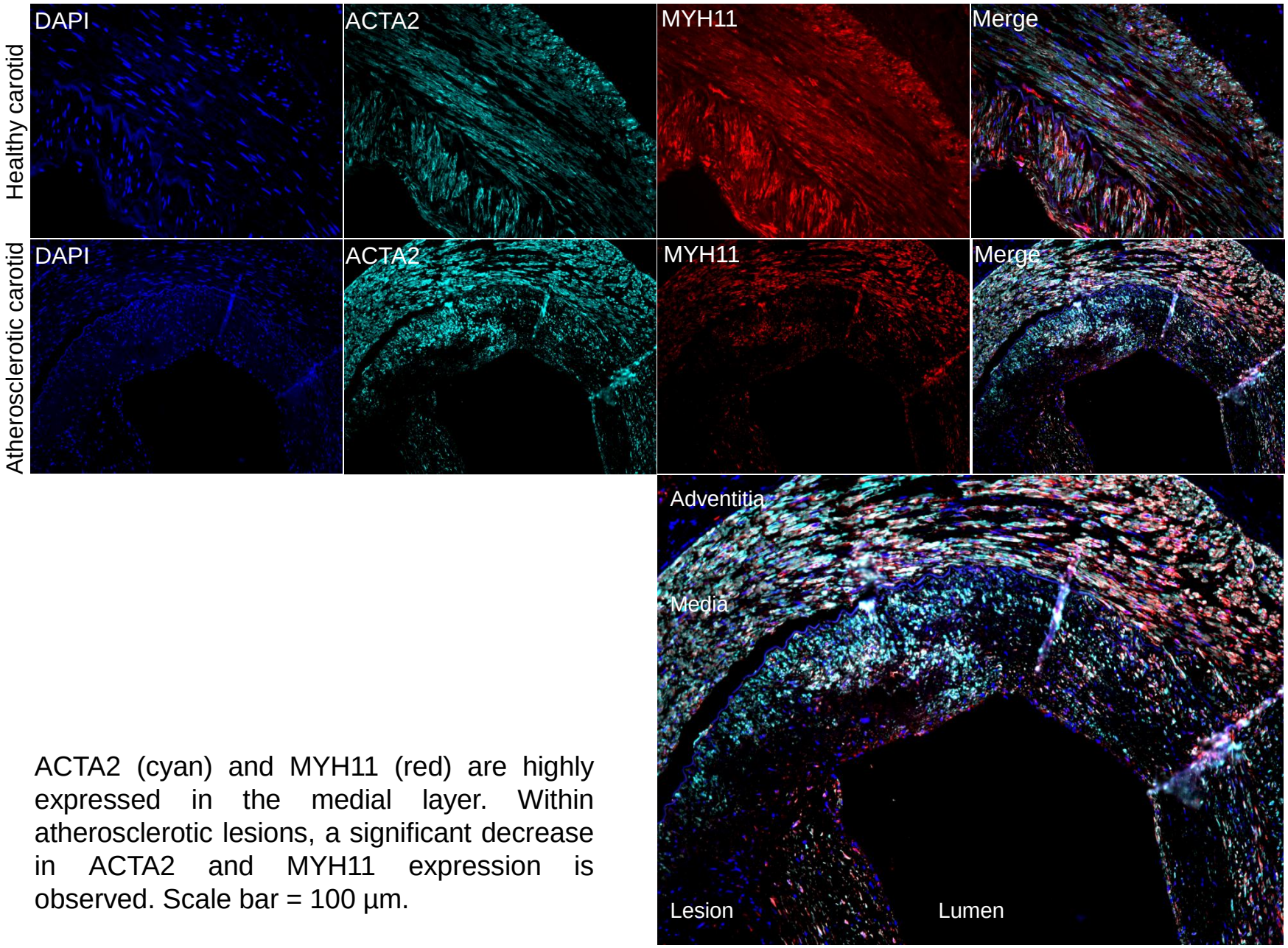

ACTA2 (cyan) and MYH11 (red) are highly expressed in the medial layer. Within atherosclerotic lesions, a significant decrease in ACTA2 and MYH11 expression is observed. Scale bar = 100 µm.

Supplementary Figure 13: MYH11 H4ac PLA in human atherosclerotic vessel tissue sections.

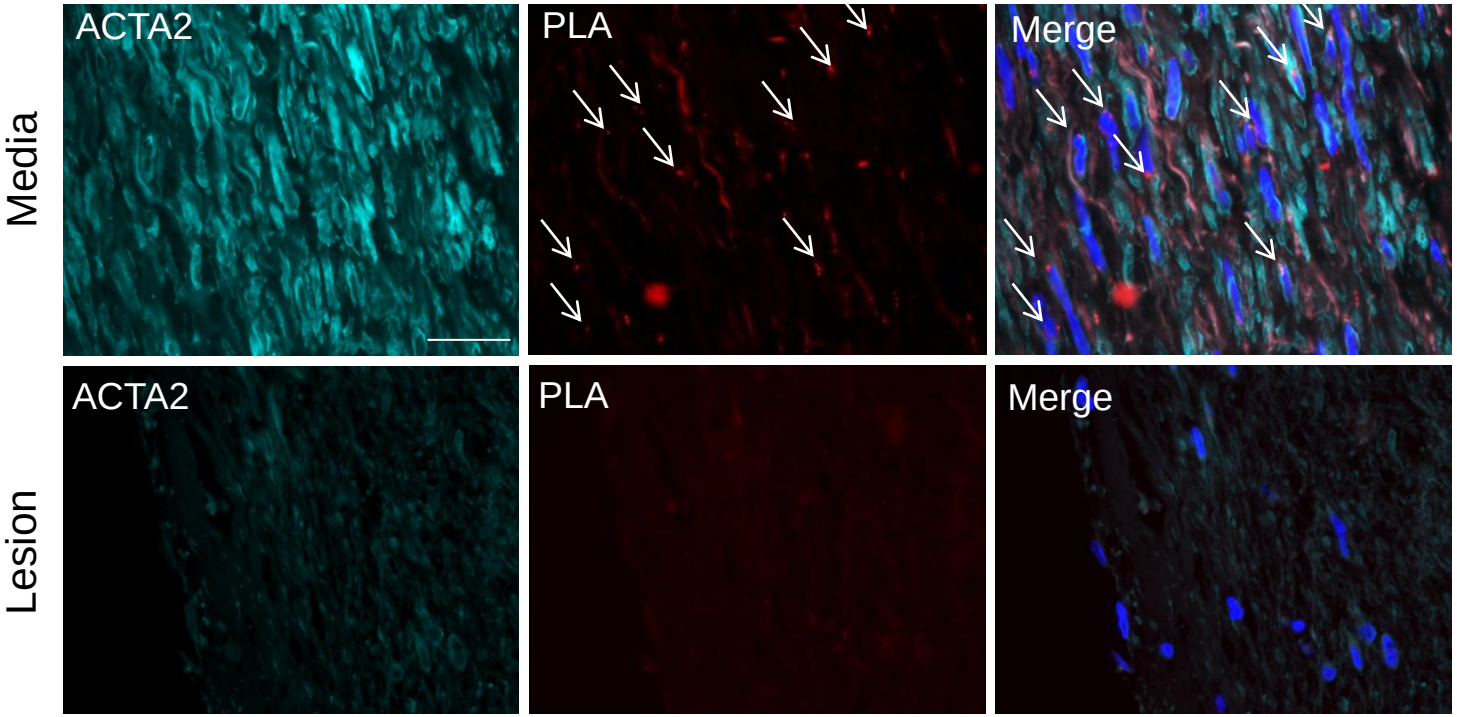

MYH11 H4ac PLA (red) combined with ACTA2 (cyan) staining within the atherosclerotic coronary artery shows that medial SMCs (ACTA2+) are *MYH11* H4ac PLA+ (arrows) whereas no *MYH11* H4ac PLA+ cells are found within the lesion. Scale bar = 50 µm.

Supplementary Table 1: Primer table

Human *MYH11* promoter	For	F1-GAGATGGCAAGTTGGGAAAA
	Rev	R1-GCTGTGGTGGATCTGACTT
	For	F2-CTCGACCCCCTTTCTCTAG
	Rev	R2-GCTGTGGTGGATCTGACTT
	For	F3-AGAGCCTGGGGAAGAGAGA
	Rev	R3- CTCGCCTAAAATTGCATTCC
Mouse *Myh11* promoter	For	F1 AGTTTGAGGCCAACGAGCTA
	Rev	R1-GCTGTGGTGGATCTGACTT
	For	F2- CCCTCCCTTTGCTAAACACA
	Rev	R2- CCAGATCCTGGGTCCTTACA
	For	F3- TAGGGTCTTAGCACGCATCC
	Rev	R3-GTCACCGCATATCCTCCAGT
	For	F4-TTCCCTCTTCCATTCCTCCT
	Rev	R4-CACTGGGCAGCAATACACAG
Mouse Myh11 cDNA	For	TGGACACCATGTCAGGGAAA
	Rev	ATGGACACAAGTGCTAAGCAGTCT
Mouse *Cdh5* promoter	For	TCCTTCTCCAGCTTGCATCT
	Rev	GAGCACAGTTGATTGCCTCA
Human *CDH5* promoter	For	TCTGAGACCCAGCAGGAAG
	Rev	GGGATGTTTCTGTTCCGTTG
Mouse *Tagln* promoter	For	AGCACCTGACTACCCACCAC
	Rev	TTTGGGCCTAACACATAGCC